

Correlating $B_q^0 \rightarrow \mu^+ \mu^-$ and $K_L \rightarrow \pi^0 \nu \bar{\nu}$ Decays with Four Generations

Wei-Shu Hou^a, Masaya Kohda^{a,b}, and Fanrong Xu^{a,c}

^aDepartment of Physics, National Taiwan University, Taipei, Taiwan 10617

^bDepartment of Physics, Chung-Yuan Christian University, Chung-Li, Taiwan 32023

^cDepartment of Physics, Jinan University, Guangzhou 510632, China

The $B_s \rightarrow \mu^+ \mu^-$ mode has finally been observed, albeit at rate 1.2σ below Standard Model (SM) value, while the rarer $B_d^0 \rightarrow \mu^+ \mu^-$ decay has central value close to 4 times SM expectation but with only 2.2σ significance. The measurement of CP violating phase ϕ_s has finally reached SM sensitivity. Concurrent with improved measurements at LHC Run 2, $K_L \rightarrow \pi^0 \nu \bar{\nu}$ and $K^+ \rightarrow \pi^+ \nu \bar{\nu}$ decays are being pursued in a similar time frame. We find, whether $B_d^0 \rightarrow \mu^+ \mu^-$ is enhanced or not, $K_L \rightarrow \pi^0 \nu \bar{\nu}$ can be enhanced up to the Grossman-Nir bound in the fourth generation model, correlated with some suppression of $B_s \rightarrow \mu^+ \mu^-$, and with ϕ_s remaining small.

PACS numbers: 14.65.Jk 12.15.Hh 11.30.Er 13.20.He

I. INTRODUCTION

The 7-and-8 TeV run (Run 1) of the LHC has been a great success, but no New Physics (NP) has emerged. The hint of NP in the forward-backward asymmetry of $B \rightarrow K^* \ell^+ \ell^-$ decay [1] from the B factories was eliminated by LHCb [2] early on. The mild hint at the Tevatron [3, 4] for *large* CP violating (CPV) phase ϕ_s in B_s^0 mixing was also swiftly eliminated by LHCb [5, 6], vanquishing the suggested possible correlation [7] with large direct CPV difference $\Delta \mathcal{A}_{K\pi} \equiv \mathcal{A}(B^+ \rightarrow K^+ \pi^0) - \mathcal{A}(B^0 \rightarrow K^+ \pi^-)$ [8]. Finally, the hot pursuit for $B_s^0 \rightarrow \mu^+ \mu^-$ at the Tevatron culminated in the recent observation by the LHCb [9] and CMS [10] experiments, albeit again consistent with the Standard Model (SM).

The combined LHC result for $B_q^0 \rightarrow \mu^+ \mu^-$ is [11],

$$\mathcal{B}(B_s^0 \rightarrow \mu^+ \mu^-) = (2.8_{-0.6}^{+0.7}) \times 10^{-9}, \quad (1)$$

$$\mathcal{B}(B_d^0 \rightarrow \mu^+ \mu^-) = (3.9_{-1.4}^{+1.6}) \times 10^{-10}. \quad (2)$$

At 6.2σ , the $B_s^0 \rightarrow \mu^+ \mu^-$ mode is established, but SM expectation is 7.6σ . The $B_d^0 \rightarrow \mu^+ \mu^-$ mode deviates from SM expectation of $(1.06 \pm 0.09) \times 10^{-10}$ [12] by 2.2σ , with central value more than 3 times the SM value. Thus, $B_d^0 \rightarrow \mu^+ \mu^-$ should be keenly followed at the up and coming LHC Run 2 (13 and 14 TeV).

The 1 fb⁻¹ LHCb update for ϕ_s [13] is:

$$\phi_s = 0.01 \pm 0.07 \pm 0.01, \quad (1 \text{ fb}^{-1}, \text{ LHCb}) \quad (3)$$

which combines two results opposite in sign,

$$\phi_s = 0.07 \pm 0.09 \pm 0.01, \quad (1 \text{ fb}^{-1} J/\psi K \bar{K}, \text{ LHCb}) \quad (4)$$

$$\phi_s = -0.14_{-0.16}^{+0.17} \pm 0.01. \quad (1 \text{ fb}^{-1} J/\psi \pi \pi, \text{ LHCb}) \quad (5)$$

Eq. (3) dominates the Heavy Flavor Averaging Group (HFAG) combination [14] of all experiments,

$$\phi_s = 0.00 \pm 0.07, \quad (\text{PDG2014}) \quad (6)$$

adopted by the Particle Data Group (PDG) [15], and is in good agreement with SM value of $\phi_s \simeq -0.04$. A preliminary result [16] of CMS,

$$\phi_s = -0.03 \pm 0.11 \pm 0.03, \quad (20 \text{ fb}^{-1}, \text{ CMS}) \quad (7)$$

is not included in PDG2014, but is fully consistent.

Also not making PDG2014 is the 3 fb⁻¹ update by LHCb for $B_s^0 \rightarrow J/\psi \pi^+ \pi^-$ with full Run 1 data [17],

$$\phi_s = 0.070 \pm 0.068 \pm 0.008, \quad (3 \text{ fb}^{-1} J/\psi \pi \pi, \text{ LHCb}) \quad (8)$$

with sign change from Eq. (5), becoming same sign with Eq. (4). Because the analysis is done simultaneously with $\Delta \Gamma_s$ measurement, the $B_s^0 \rightarrow J/\psi K \bar{K}$ mode took much longer. Intriguingly, it also switched sign [18],

$$\phi_s = -0.058 \pm 0.049 \pm 0.006, \quad (3 \text{ fb}^{-1} J/\psi \phi, \text{ LHCb}) \quad (9)$$

and the combined 3 fb⁻¹ result is,

$$\phi_s = -0.010 \pm 0.039, \quad (3 \text{ fb}^{-1}, \text{ LHCb}) \quad (10)$$

with no indication of New Physics.

A third measurement of interest by LHCb is the so-called P'_5 anomaly. The significance (3.7σ), however, did not change from 1 fb⁻¹ [19] to 3 fb⁻¹ [20]. Given that this is one out of many angular variables in $B^0 \rightarrow K^{*0} \mu^+ \mu^-$, it remains to be seen whether the “anomaly” is genuine. Unfortunately, it will take several years to accumulate and analyze an equivalent amount of data at Run 2. We note in passing the so-called R_K anomaly [21] in lepton universality violation in $B^+ \rightarrow K^+ \ell^+ \ell^-$ decays, which has 2.6σ deviation from SM expectation. It may or may not be related to the P'_5 anomaly.

What are the prospects for Run 2? A total of 8 fb⁻¹ or more data is expected by LHCb up to 2018. Data rate is much higher for CMS, but trigger bandwidth is an issue. The Belle II experiment should be completed in this time frame in Japan. Though not particularly competitive in ϕ_s and $B_q^0 \rightarrow \mu^+ \mu^-$, it could crosscheck P'_5 . Given that the two former measurables correspond to $b \leftrightarrow s$ and $b \rightarrow d$ transitions, one involving CPV, the other not, there is one particular process that comes to mind: $K \rightarrow \pi \nu \bar{\nu}$ decays, which are $s \rightarrow d$ transitions. The neutral $K_L^0 \rightarrow \pi^0 \nu \bar{\nu}$ decay, pursued by the KOTO experiment [22] in Japan, is purely CPV. The charged $K^+ \rightarrow \pi^+ \nu \bar{\nu}$ mode is pursued by the NA62 experiment [23] at CERN. Both experiments run within a similar time frame. If one has

indications for NP in $B_q^0 \rightarrow \mu^+ \mu^-$ and/or ϕ_s , likely one would find NP in $K \rightarrow \pi \nu \bar{\nu}$, and *vice versa*. An element of competition between high- and low-energy luminosity frontiers would be quite interesting.

In this letter we study the *correlations* between the measurables $B_d^0 \rightarrow \mu^+ \mu^-$, $B_s^0 \rightarrow \mu^+ \mu^-$, ϕ_s , and $K \rightarrow \pi \nu \bar{\nu}$ (especially $K_L^0 \rightarrow \pi^0 \nu \nu$), in the 4th generation (4G) model, which cannot address P_5/R_K anomalies. It was pointed out quite some time ago [24] that 4G can bring about an enhanced $K_L^0 \rightarrow \pi^0 \nu \nu$, and now that KOTO is running, one should check whether it remains true. Although some may now find 4G extreme, our aim is towards enhanced $B_d^0 \rightarrow \mu^+ \mu^-$ rate by a factor of three and still survive all *flavor* constraints. The issue with 4G is the observation of a light Higgs boson, without the anticipated factor of 9 enhancement in cross section. On one hand it has been argued [25] that there still exists other interpretation of this 125 GeV boson, that is to identify it as dilaton from a 4G theory with strong Yukawa interaction. On the other hand, Higgs boson practically does not enter (i.e. is “orthogonal” to) low energy flavor changing processes, and, *if* one discovers an enhanced $B_d^0 \rightarrow \mu^+ \mu^-$ decay [26], it may put some doubt on the Higgs nature of the observed 125 GeV particle. We view the issue, different interpretation of this boson, is still opens and would be settled by 2018. Our 4G study serves to illustrate how New Physics in $B_q^0 \rightarrow \mu^+ \mu^-$, ϕ_s , and $K \rightarrow \pi \nu \bar{\nu}$ might be accommodated.

In what follows, we give the formulas and data inputs, then our numerical results and end with some discussions.

II. FORMULAS AND DATA INPUT

We define the parameters $x_q = m_q^2/M_W^2$, $\lambda_q^{ds} \equiv V_{qd}V_{qs}^*$ ($q = u, c, t, t'$), with

$$V_{t'd}^* V_{t's} \equiv (\lambda_{t'}^{ds})^* \equiv r_{ds} e^{i\phi_{ds}}. \quad (11)$$

We adopt the parametrization of Ref. [27] for the 4×4 CKM matrix, with convention and treatment of Ref. [24]. In particular, we assume SM-like values for s_{12} , s_{23} , s_{13} and $\phi_{ub} \simeq \gamma/\phi_3$, with following input: $|V_{us}| = 0.2252 \pm 0.0009$, $|V_{cb}| = 0.0409 \pm 0.0011$, $|V_{ub}^{\text{ave}}| = (4.15 \pm 0.49) \times 10^{-3}$, $\gamma/\phi_3 = (68_{-11}^{+10})^\circ$. This is a simplification, since we try to observe trends, rather than making a full fit. We find taking the “exclusive” measurement value for $|V_{ub}|$ allows less enhancement range for $K_L \rightarrow \pi^0 \nu \bar{\nu}$.

Having a 4th generation of quarks brings in three new angles and two new phases. In this paper, we take

$$m_{t'} = 1000 \text{ GeV}, \quad s_{34} \simeq m_W/m_{t'} \simeq 0.08, \quad (12)$$

for sake of illustration, thereby fixing one of the angles. A second angle and one of the two phases are fixed by the discussion illustrated below. We are then left with two mixing parameters, and for our interest in $K \rightarrow \pi \nu \bar{\nu}$ decays, we take as r_{ds} and ϕ_{ds} in Eq. (11). Our choice [28] of $m_{t'} = 1000 \text{ GeV}$ is above the experimental bound [15],

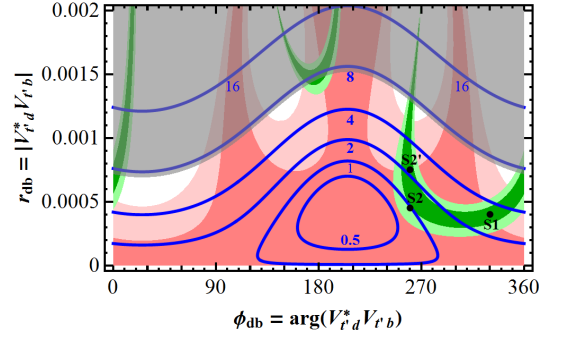


FIG. 1. Update of Fig. 3(a) of Ref. [26], taking $|V_{ub}^{\text{ave}}|$ and $m_{t'} = 1000 \text{ GeV}$. The pink-shaded contours correspond to $1(2)\sigma$ regions of Δm_{B_d} allowed by $f_{B_d} = (190.5 \pm 4.2) \text{ MeV}$ while the green-shaded bands are for $1(2)\sigma$ in $\sin 2\beta/\phi_1 = 0.682 \pm 0.019$ [14]. Solid-blue lines are labeled $10^{10} \mathcal{B}(B_d \rightarrow \mu^+ \mu^-)$ contours, with upper bound of 7.4 [9] applied. Marked points S1, S2, S2' are explained in text.

which is beyond the nominal [29] unitarity bound. Even with vector-like 4G quarks, the experimental bound has reached beyond 700 GeV [15]. We adhere to sequential 4G to reduce the number of parameters.

We have suggested [26] that an enhanced $B_d \rightarrow \mu^+ \mu^-$ could indicate the presence of 4G, while suppression of $B_s \rightarrow \mu^+ \mu^-$ could also be accommodated [30]. These are supported by current data [11], but more data is clearly needed. In Fig. 1, we update Fig. 3(a) of Ref. [26] on the $r_{db}-\phi_{db}$ plane, where $V_{t'd}^* V_{t'b} \equiv r_{db} e^{i\phi_{db}}$. We use the FLAG [31] average of $N_f = 2 + 1$ lattice results $f_{B_d} = (190.5 \pm 4.2) \text{ MeV}$, $f_{B_d} \hat{B}_{B_d}^{1/2} = (216 \pm 15) \text{ MeV}$. We no longer take the ratio with Δm_{B_d} for $B_d \rightarrow \mu^+ \mu^-$ branching ratios, but update the constraints: $\sin 2\beta/\phi_1 = 0.682 \pm 0.019$ (HFAG Winter 2014 [14]), $\mathcal{B}(B_d \rightarrow \mu^+ \mu^-) < 7.4 \times 10^{-10}$ (95% CL limit of LHCb [9]). The latter is softer than the recent CMS and LHCb combination of Eq. (2).

From Fig. 1, we shall consider two scenarios

$$r_{db} e^{i\phi_{db}} = 0.00040 e^{i330^\circ}, 0.00045 e^{i260^\circ}, \quad (13)$$

marked as S1, S2 in Fig. 1, to illustrate

$$\mathcal{B}(B_d \rightarrow \mu^+ \mu^-) \sim 3 \times 10^{-10}, 1 \times 10^{-10}, \quad (14)$$

where we stay within 1σ boundaries of *both* Δm_{B_d} (uncertainty in f_{B_d}) and $\sin 2\beta/\phi_1$. $B_d \rightarrow \mu^+ \mu^-$ is SM-like for S2, but carries a near maximal 4G CPV phase ϕ_{db} . The point S2' will be discussed towards the end.

For $b \rightarrow s$ observables, we update both formulas and input parameters of Ref. [32]. For the CPV phase $\phi_s \equiv 2\Phi_{B_s}$ in $B_s-\bar{B}_s$ mixing, we use [33] $2\Phi_{B_s} = \arg \Delta_{12}^s$ with $\Delta_{12}^s = (\lambda_t^{bs})^2 S_0(x_t) + 2\lambda_t^{bs} \lambda_{t'}^{bs} S_0(x_t, x_{t'}) + (\lambda_{t'}^{bs})^2 S_0(x_{t'})$, where $\lambda_q^{bs} \equiv V_{qs}^* V_{qb}$ ($q = t, t'$). We adopt the ϕ_s value of Eq. (10) and impose $1(2)\sigma$ constraints.

For $\mathcal{B}(B_s \rightarrow \mu^+ \mu^-)$, because $\Delta\Gamma_s$ is sizable, experimental results should be compared with the $\Delta\Gamma_s$ -corrected [34] branching ratio denoted with a bar,

$$\bar{\mathcal{B}}(B_s \rightarrow \mu^+ \mu^-) = \frac{1 - y_s^2}{1 + A_{\Delta\Gamma}^{\mu\mu} y_s} \mathcal{B}(B_s \rightarrow \mu^+ \mu^-), \quad (15)$$

where $y_s = \Delta\Gamma_s/2\Gamma_s = 0.069 \pm 0.006$ [15], $A_{\Delta\Gamma}^{\mu\mu} = \cos[2 \arg(C_{10}) - 2\Phi_{B_s}]$, and [33]

$$\mathcal{B}(B_s \rightarrow \mu^+ \mu^-) = \tau_{B_s} \frac{G_F^2}{\pi} \left(\frac{\alpha}{4\pi \sin^2 \theta_W} \right)^2 f_{B_s}^2 m_\mu^2 m_{B_s} \times \sqrt{1 - 4m_\mu^2/m_{B_s}^2} \eta_{\text{eff}}^2 |\lambda_t^{bs} Y_0(x_t) + \lambda_{t'}^{bs} Y_0(x_{t'})|^2. \quad (16)$$

We use $\eta_{\text{eff}} = 0.9882 \pm 0.0024$ which is at NNLO for QCD and NLO for electroweak corrections [35], and we use the FLAG [31] average of $N_f = 2 + 1$ lattice results $f_{B_s} = (227.7 \pm 4.5)$ MeV and $f_{B_s} \hat{B}_{B_s}^{1/2} = (266 \pm 18)$ MeV, where the latter enters B_s -mixing. We use Eq. (1) and impose $1(2)\sigma$ experimental constraints, which is much larger than the hadronic uncertainty.

We find that Δm_{B_s} does not give further constraints in the parameter space of our interest, within hadronic uncertainty of f_{B_s} . The ratio $\Delta m_{B_s}/\Delta m_{B_d}$ has reduced hadronic uncertainty, as can be read from $\xi \equiv f_{B_s} \hat{B}_{B_s}^{1/2}/f_{B_d} \hat{B}_{B_d}^{1/2} = 1.268 \pm 0.063$ [31], hence provides stronger constraint than individual Δm_{B_s} or Δm_{B_d} .

For $K^+ \rightarrow \pi^+ \nu \bar{\nu}$ and $K_L \rightarrow \pi^0 \nu \bar{\nu}$, we use the formulas of Ref. [24] and update input parameters: $m_t(m_t) = 163$ GeV [36], $\kappa_+ = (5.173 \pm 0.025) \times 10^{-11} \times (|V_{us}|/0.225)^8$ and $\kappa_L = (2.231 \pm 0.013) \times 10^{-10} \times (|V_{us}|/0.225)^8$ [37], and $P_c(X) = 0.41 \pm 0.05$ [38]. We impose $\mathcal{B}(K^+ \rightarrow \pi^+ \nu \bar{\nu})_{\text{exp}} < 3.35 \times 10^{-10}$ (90% C.L. from E949 [39]), implying the Grossman-Nir (GN) bound [40]

$$\begin{aligned} \mathcal{B}(K_L \rightarrow \pi^0 \nu \bar{\nu}) &< \frac{\kappa_L}{\kappa_+} \mathcal{B}(K^+ \rightarrow \pi^+ \nu \bar{\nu}) \\ &\lesssim 1.4 \times 10^{-9}, \end{aligned} \quad (17)$$

which is stronger than the direct limit by E391a [41].

For Short-Distance (SD) contribution to $K_L \rightarrow \mu^+ \mu^-$,

$$\begin{aligned} \mathcal{B}(K_L \rightarrow \mu^+ \mu^-)_{\text{SD}} &= \kappa_\mu |V_{us}|^{-10} [\text{Re} \lambda_c^{ds} |V_{us}|^4 P_c(Y) \\ &+ \text{Re} \lambda_t^{ds} \eta_Y Y_0(x_t) + \text{Re} \lambda_{t'}^{ds} \eta_Y Y_0(x_{t'})]^2, \end{aligned} \quad (18)$$

we use $\kappa_\mu = (2.009 \pm 0.017) \times 10^{-9} \times (|V_{us}|/0.225)^8$, $P_c(Y) = (0.115 \pm 0.018) \times (0.225/|V_{us}|)^4$ [42], and $Y_0(x)$ as given in Ref. [33]. With the common QCD correction factor $\eta_Y = 1.012$, we adopt the estimate [43] $\mathcal{B}(K_L \rightarrow \mu^+ \mu^-)_{\text{SD}} \leq 2.5 \times 10^{-9}$ as upper bound.

For $K \rightarrow \pi\pi$ indirect CP violation, we use [33].

$$\varepsilon_K = \frac{\kappa_\varepsilon e^{i\varphi_\varepsilon}}{\sqrt{2}(\Delta m_K)_{\text{exp}}} \text{Im}(M_{12}^K), \quad (19)$$

$$\begin{aligned} (M_{12}^K)^* &= \frac{G_F^2 M_W^2}{12\pi^2} m_K f_K^2 \hat{B}_K [(\lambda_c^{ds})^2 \eta_{cc} S_0(x_c) \\ &+ (\lambda_t^{ds})^2 \eta_{tt} S_0(x_t) + 2\lambda_c^{ds} \lambda_t^{ds} \eta_{ct} S_0(x_c, x_t) \\ &+ (\lambda_{t'}^{ds})^2 \eta_{t't'} S_0(x_{t'}) + 2\lambda_c^{ds} \lambda_{t'}^{ds} \eta_{ct'} S_0(x_c, x_{t'}) \\ &+ 2\lambda_t^{ds} \lambda_{t'}^{ds} \eta_{tt'} S_0(x_t, x_{t'})], \end{aligned} \quad (20)$$

where $(\Delta m_K)_{\text{exp}} = (5.293 \pm 0.009) \times 10^9 \text{ s}^{-1}$ [15], $\varphi_\varepsilon = (43.52 \pm 0.05)^\circ$ [15] and $\kappa_\varepsilon = 0.94 \pm 0.02$ [44]. We use $\eta_{cc} = 1.87 \pm 0.76$ [45], $\eta_{tt} = 0.5765 \pm 0.0065$ [46, 47], $\eta_{ct} = 0.496 \pm 0.047$ [47] and approximate $\eta_{tt} = \eta_{t't'} = \eta_{t't'}$, $\eta_{ct} = \eta_{ct'}$. Theoretical uncertainty is around 11% [48], far larger than experimental error [15]: $|\varepsilon_K| = (2.228 \pm 0.011) \times 10^{-3}$ and $\text{Re}(\varepsilon_K) > 0$. We thus impose ε_K to be within $\pm 11\%$ from data.

Direct CP violation in $K \rightarrow \pi\pi$ is affected even more by hadronic uncertainties. We use [24]

$$\frac{\varepsilon'}{\varepsilon} = a [\text{Im}(\lambda_c^{ds}) P_0 + \text{Im}(\lambda_t^{ds}) F(x_t) + \text{Im}(\lambda_{t'}^{ds}) F(x_{t'})],$$

where $a = 0.92 \pm 0.03$ [49] is a correction from $\Delta I = 5/2$ transitions [50]. The function $F(x)$, which relies on hadronic parameters R_6 and R_8 ¹, is defined as $F(x) = P_X X_0(x) + P_Y Y_0(x) + P_Z Z_0(x) + P_E E_0(x)$ with $P_i = r_i^{(0)} + r_i^{(6)} R_6 + r_i^{(8)} R_8$ ($i = 0, X, Y, Z, E$). We also update numerical values for the coefficients $r_i^{(0)}$, $r_i^{(6)}$ and $r_i^{(8)}$, for $\alpha_s(M_Z) = 0.1185$ [15] given in Table 1 of Ref. [49], by reversing the sign of $r_0^{(j)}$ as done in Ref. [24]. We take $R_8 = 0.7$ from lattice [51], with the translation by Ref. [49]. There is still no reliable result from lattice QCD for R_6 , so we treat [24, 52] it as a parameter. That is, for each value of $R_6 = 1.0, 1.5, 2.0, 2.5$, we require ε'/ε to agree within 1σ experimental error [15],

$$\frac{\varepsilon'}{\varepsilon} \simeq \text{Re} \left(\frac{\varepsilon'}{\varepsilon} \right) = (1.66 \pm 0.23) \times 10^{-3}. \quad (21)$$

Comments on other potentially important observables are in order. In contrast to $\Delta m_{B_{d,s}}$, Δm_K is polluted by Long-Distance (LD) effects. We have checked that there is no significant change of the SD part from the SM value and $(\Delta m_K)_{\text{SD}}$ is still below the measured value. D^0 - \bar{D}^0 mixing is also subject to LD effects. We checked that the SD contribution to the mixing amplitude M_{12}^D from b' (with $m_{b'} \sim m_{t'}$) could be enhanced up to 3 times the

¹ Furthermore, the relations between hadronic parameters $R_{6,8}$ and bag parameters $B_6^{(1/2)}$ and $B_8^{(3/2)}$ which are calculated in Lattice QCD, are $R_6 = 1.13 B_6^{(1/2)} \left[\frac{114 \text{ MeV}}{m_s(m_c) + m_d(m_c)} \right]^2$ and $R_8 = 1.13 B_8^{(3/2)} \left[\frac{114 \text{ MeV}}{m_s(m_c) + m_d(m_c)} \right]^2$, see [49].

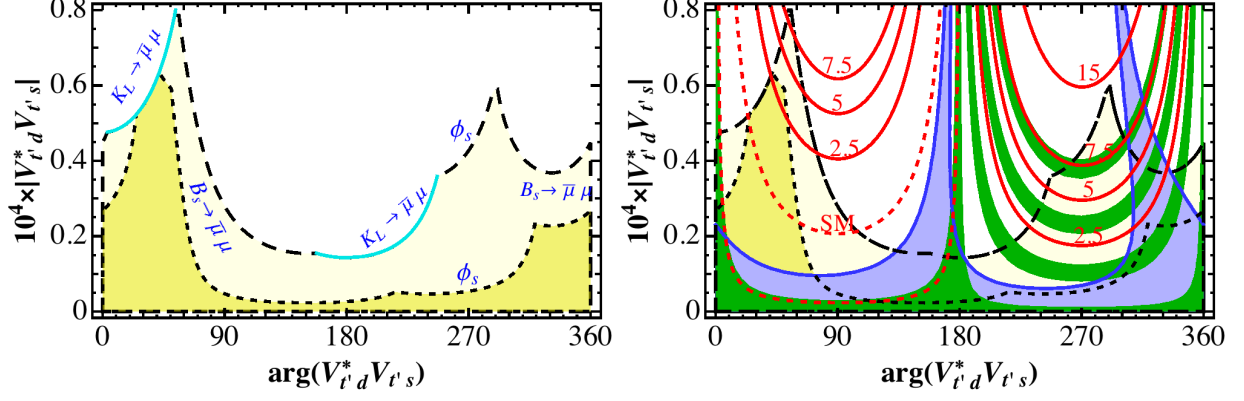


FIG. 2. [left] Allowed region in $|V_{t'd}^* V_{t's}| - \arg(V_{t'd}^* V_{t's})$ (i.e. $r_{ds} - \phi_{ds}$) plane for Scenario S1, $r_{db} e^{i\phi_{db}} = 0.0004 e^{i330^\circ}$ (enhanced $B_d \rightarrow \mu^+ \mu^-$) and $\phi_s = -0.010 \pm 0.039$ (Eq. (10)), where the constraint source for each boundary is indicated. The leading constraint is $B_s \rightarrow \mu^+ \mu^-$, where $1(2)\sigma$ region — towards larger (smaller) BR in central region (4th-extending-to-1st quadrants) — is (very) light shaded, separated by dashed lines, except: $K_L \rightarrow \mu^+ \mu^-$ cuts off at upper left, as well as center-right, indicated by light-blue solid lines; $1(2)\sigma$ allowed ϕ_s cuts off the $1(2)\sigma$ allowed $B_s \rightarrow \mu^+ \mu^-$ in right-center, plus a sliver in 1st quadrant. [right] The allowed region is further overlaid with ε_K (blue-shaded), ε'/ε (narrow green bands corresponding to R_6 in increasing order from 1.0, 1.5, 2.0, 2.5) and $\mathcal{B}(K_L \rightarrow \pi^0 \nu \nu)$, labeled in 10^{-10} units. The illustration is for $m_{t'} = 1000$ GeV (Eq. (11)).

SM value in the parameter space of our interest, but it is still well below the measured value of Δm_D .

$B \rightarrow K^{(*)} \mu^+ \mu^-$ observables are subject to precise measurements at the LHC and severely constrain NP effects. We checked that the 4G t' effects on C_9 is within 5% of the SM value (~ 4.3) in our parameter space. The 4G effects on C_{10} can be as large as unity in some part of the target parameter space. However, adopting the model independent constraint in Ref. [53], we checked that the changes are within 2σ for various modes. It cannot explain P'_5 , nor R_K , anomalies.

III. RESULTS

To illustrate the connection between $B_d \rightarrow \mu^+ \mu^-$ and $K_L \rightarrow \pi^0 \nu \bar{\nu}$, we explore two scenarios (see Fig. 1):

- Scenario S1: $r_{db} e^{i\phi_{db}} = 0.00040 e^{i330^\circ}$
 $\mathcal{B}(B_d \rightarrow \mu^+ \mu^-) \gtrsim 3 \times \text{SM}$, with $e^{i\phi_{db}}$ complex;
- Scenario S2: $r_{db} e^{i\phi_{db}} = 0.00045 e^{i260^\circ}$
 $\mathcal{B}(B_d \rightarrow \mu^+ \mu^-) \sim \text{SM}$, ϕ_{db} is near maximal CPV;

With formulas and data input given in Sec. II, we plot in Fig. 2[left] the region in the $|V_{t'd}^* V_{t's}| - \arg(V_{t'd}^* V_{t's})$ or $r_{ds} - \phi_{ds}$ plane allowed by various constraints for S1. The golden-hued (very) light shaded regions are for $1(2)\sigma$ of the $B_s \rightarrow \mu^+ \mu^-$ mode. Other constraints, labeled by the process, cut in at certain regions: $\mathcal{B}(K_L \rightarrow \mu \mu)_{\text{SD}}$ at the upper-left corner, and just right of center; $\phi_s = -0.049(-0.088)$ at $1(2)\sigma$ cuts off near center of right-hand side, and a tiny sliver in first quadrant. The remaining 1σ contours for $B_s \rightarrow \mu^+ \mu^-$ correspond to 3.5×10^{-9} (central-left region) and 2.2×10^{-9} (4th quadrant extending into 1st quadrant) in rate, and for 2σ contours,

4.3×10^{-9} [11] from 1st to 2nd quadrant and 1.6×10^{-9} in 4th quadrant only. We find that $R = \Delta m_{B_d} / \Delta m_{B_s}$ does not provide further constraint within 2σ .

The allowed region of Fig. 2[left] is further overlaid, in Fig. 2[right], by the constraints of ε_K , ε'/ε , and give $K_L \rightarrow \pi^0 \nu \nu$ contours in red-solid, labeled by BR values in 10^{-10} units. Note that “15” is just above the nominal GN bound of Eq. (17), while the region $\lesssim \text{SM}$ strength is marked by red-dash lines with label “SM”. The ε_K constraint, plotted in shaded blue with theoretical error (experimental error negligible), prefers small $|V_{t'd}^* V_{t's}|$ values, except two “chimneys” where the phase of $V_{t'd}^* V_{t's}$ is small for one near 180° , and the other is tilted in the fourth quadrant. The ε'/ε constraint is more subtle, because of the less known [52] hadronic parameter R_6 (we fix $R_8 \simeq 0.7$ [51]). We illustrate [24] with $R_6 = 1.0, 1.5, 2.0, 2.5$, in ascending order of green bands determined by experimental error of ε'/ε .

First, we observe that the ε_K and ε'/ε constraints disfavor the possible enhancements for $K_L \rightarrow \pi^0 \nu \nu$ when $\arg(V_{t'd}^* V_{t's})$ is in the first two quadrants. Second, if one keeps all constraints to 1σ , then $K_L \rightarrow \pi^0 \nu \nu$ could reach a factor ~ 7 above SM, with modest R_6 values. However, if one allows larger R_6 (up to 2.5) as well as 2σ variations, the ε_K “chimney” in the 4th quadrant allows $K_L \rightarrow \pi^0 \nu \nu$ to be enhanced up to $1/3$, even $1/2$, the GN bound. There is a correlation between larger $K_L \rightarrow \pi^0 \nu \nu$ and smaller $B_s \rightarrow \mu \mu$. If KOTO observes $K_L \rightarrow \pi^0 \nu \nu$ shortly after reaching below the GN bound, a rather large R_6 value could be implied. One argument for larger $K_L \rightarrow \pi^0 \nu \nu$ or smaller $B_s \rightarrow \mu \mu$ is for larger values of $|V_{t'd}^* V_{t's}|$: since $|V_{t'd}| \sim 0.005$, to have $|V_{t's}| > |V_{t'd}|$ would demand $|V_{t'd}^* V_{t's}| \gtrsim 0.25 \times 10^{-4}$.

We see the prowess, still, of the various kaon measurements, with $K_L \rightarrow \pi^0 \nu \nu$ as the main frontier ($K^+ \rightarrow$

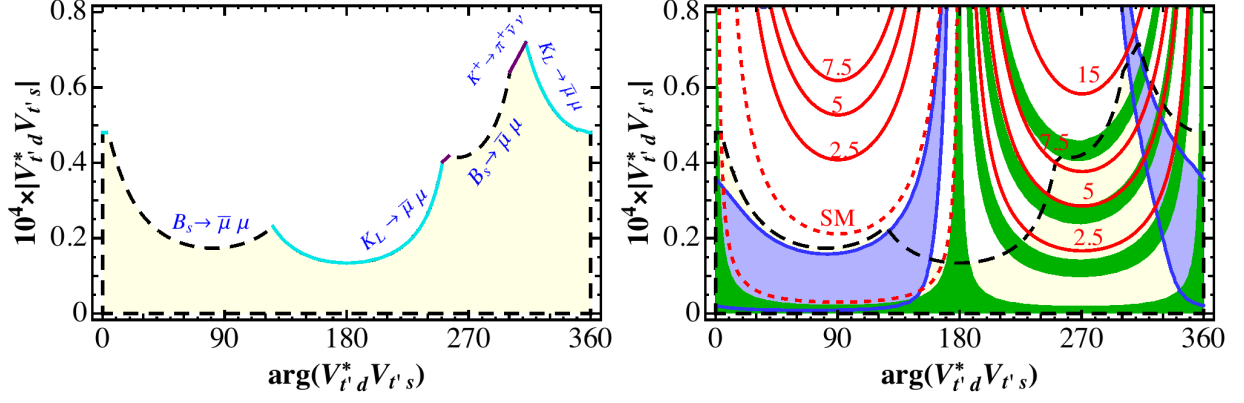


FIG. 3. Scenario S2, $r_{db} e^{i\phi_{db}} = 0.00045 e^{i260^\circ}$ (SM-like $B_d \rightarrow \mu^+ \mu^-$): [left] Similar to Fig. 2a, where for the 4th quadrant of interest, the 2σ dashed line is for $B_s \rightarrow \mu^+ \mu^-$ and solid is for $K_L \rightarrow \mu^+ \mu^-$ (plus a bit from $K^+ \rightarrow \pi^+ \nu \bar{\nu}$); [right] Similar to Fig. 2b, with ε_K (blue-shaded) ε'/ε (green bands) and $K_L \rightarrow \pi^0 \nu \bar{\nu}$ (red labelled contours) overlaid.

$\pi^+ \nu \bar{\nu}$ did not enter discussion), on a par with the ongoing $B_{d,s} \rightarrow \mu\mu$ and ϕ_s measurement efforts.

For Scenario S2, where $B_d \rightarrow \mu\mu$ is taken as consistent with SM, but $\phi_{db} \equiv \arg(V_{t'd}^* V_{t'b}) \simeq 260^\circ$ is close to maximal CPV phase (in our convention, $V_{t'b}$ is real) with $K_L \rightarrow \pi^0 \nu \bar{\nu}$ in mind, we plot in Fig. 3[left] the results corresponding to Fig. 2[left]. The regions marked by long dashed lines and very lightly shaded are all beyond 1σ level, indicating more tension, including in $R = \Delta m_{B_d}/\Delta m_{B_s}$. The $B_s \rightarrow \mu\mu$ constraint at 2σ is interspersed with the $\mathcal{B}(K_L \rightarrow \mu\mu)_{\text{SD}}$ constraint, plus short segments from $K^+ \rightarrow \pi^+ \nu \bar{\nu}$. As in Fig. 2[right], we overlay the constraints of ε_K , ε'/ε , as well as $K_L \rightarrow \pi^0 \nu \bar{\nu}$ contours, in Fig. 3[right]. Again, $K_L \rightarrow \pi^0 \nu \bar{\nu}$ cannot get enhanced in first two quadrants. For the blue-shaded “chimney” in 4th quadrant, as the R_6 value rises, $K_L \rightarrow \pi^0 \nu \bar{\nu}$ could get enhanced even up to GN bound, but $B_s \rightarrow \mu\mu$ would become relatively suppressed, and there is some tension with SD contribution to $K_L \rightarrow \mu\mu$. Note that $\mathcal{B}(B_d \rightarrow \mu\mu) \sim \text{SM}$ in this case. Here, having $|V_{t's}| > |V_{t'd}|$ would demand $|V_{t'd}^* V_{t's}| \gtrsim 0.32 \times 10^{-4}$, hence in favor of larger $K_L \rightarrow \pi^0 \nu \bar{\nu}$.

We have marked a point S2' in Fig. 1, which has same $\phi_{db} \simeq 260^\circ$ as S2, but enhances $B_d \rightarrow \mu\mu$ by a larger $r_{db} \equiv |V_{t'd}^* V_{t'b}| \simeq 0.00075$. The trouble with S2' is that $\Delta m_{B_d}/\Delta m_{B_s}$ ratio becomes inconsistent at 2σ level, which we do not consider as viable. However, from S2 towards S2', one could enhance $B_d \rightarrow \mu\mu$ while $K_L \rightarrow \pi^0 \nu \bar{\nu}$ is more easily enhanced up to GN bound. The cost would be some tension in $\Delta m_{B_d}/\Delta m_{B_s}$.

In all these discussions, ϕ_s is well within range of the 3 fb^{-1} result of LHCb, Eq. (10).

IV. DISCUSSION AND CONCLUSION

We are interested in the correlation between $B_d \rightarrow \mu^+ \mu^-$ and $K_L \rightarrow \pi^0 \nu \bar{\nu}$ in 4G, as constrained by $B_s \rightarrow \mu\mu$

and ϕ_s . Scenario S1 illustrates enhanced $B_d \rightarrow \mu^+ \mu^-$ with generic $V_{t'd}^* V_{t'b}$. Every measurement other than $B_d \rightarrow \mu^+ \mu^-$ would be close to SM expectation, and a mild enhancement of $K_L \rightarrow \pi^0 \nu \bar{\nu}$ is possible. But it would take some while for KOTO to reach this sensitivity. Larger $K_L \rightarrow \pi^0 \nu \bar{\nu}$ correlates with smaller $B_s \rightarrow \mu^+ \mu^-$, as well as larger hadronic parameter R_6 . The ϕ_s constraint basically suppresses the phase of $V_{t's}^* V_{t'b}$.

It could happen that $B_d \rightarrow \mu^+ \mu^-$ ends up SM-like, which is illustrated by Scenario S2. In the 4G framework that accounts (within 1σ) for the $\sin 2\beta/\phi_1$ “anomaly”, this occurs when $\phi_{db} \equiv \arg(V_{t'd}^* V_{t'b})$ phase is near maximal, which is of interest for enhancing $K_L \rightarrow \pi^0 \nu \bar{\nu}$, a purely CPV process. We find that $K_L \rightarrow \pi^0 \nu \bar{\nu}$ can be enhanced up to practically the GN bound at the cost of large R_6 , while staying within the ϕ_s constraint. There is the same correlation of larger $K_L \rightarrow \pi^0 \nu \bar{\nu}$ for smaller $B_s \rightarrow \mu^+ \mu^-$. While the S2' point would push $\Delta m_{B_d}/\Delta m_{B_s}$ beyond 2σ tolerance, some $|V_{t'd}^* V_{t'b}| \equiv r_{db}$ value below 0.00075 could still enhance $B_d \rightarrow \mu^+ \mu^-$ a bit from SM, but $K_L \rightarrow \pi^0 \nu \bar{\nu}$ can more easily saturate the Grossman-Nir bound, with implication that $K^+ \rightarrow \pi^+ \nu \bar{\nu}$ is towards the large side allowed by E949, $B_s \rightarrow \mu\mu$ is visibly suppressed, while R_6 must be sizable. This would clearly be a bonanza situation for faster discovery!

We have used 4G for illustration [28], since it supplies $V_{t's}$ and $V_{t'd}$ that affect $b \rightarrow s$ and $b \rightarrow d$ transitions, and induces correlations with $s \rightarrow d$ transitions. It is generally viewed that the fourth generation is ruled out by the SM-like Higgs boson production cross section. But we have argued [26] that the Higgs boson does not enter the low energy processes discussed here, hence these processes are independent *flavor* checks. Furthermore, loopholes exist for the SM-Higgs interpretation [25].

If one does not accept 4G, we stress that $B_d \rightarrow \mu^+ \mu^-$ may well turn out have enhanced rate. Whatever new flavor physics one resorts to, there is the myriad of constraints of Sec. II. We believe no model can survive intact and “without blemish” [54]. Thus, the modes

$B_{d,s} \rightarrow \mu^+\mu^-$, ϕ_s and $K_L \rightarrow \pi^0\nu\nu$ provide “pressure tests” to our understanding of flavor and CP violation, where genuine surprises may emerge. Though differences must exist, we believe there would be correlations between the above four modes in any New Physics model with a limited set of new parameters. The NA62 experiment has started [23] running. If $K^+ \rightarrow \pi^+\nu\nu$ turns out to be above the 90% CL limit from E949, the GN bound for $K_L \rightarrow \pi^0\nu\nu$ moves up, making things more interesting for KOTO, where the aim [22] for the 2015 run is to reach the GN bound around 1.4×10^{-9} .

In conclusion, enhanced $B_d^0 \rightarrow \mu^+\mu^-$ could correlate with enhanced $K_L \rightarrow \pi^0\nu\bar{\nu}$ up to the Grossman-Nir bound in the 4th generation model. $B_s^0 \rightarrow \mu^+\mu^-$ becomes somewhat suppressed, with CPV phase $\phi_s \simeq 0$. Together with $K^+ \rightarrow \pi^+\nu\bar{\nu}$, these measurements would

provide “pressure tests” to our understanding of flavor and CP violation for any New Physics model. They should be followed earnestly in parallel to the scrutiny of the nature of the 125 GeV boson at LHC Run 2.

Acknowledgement. WSH is supported by the the Academic Summit grant NSC 103-2745-M-002-001-ASP of the National Science Council, as well as by grant NTU-EPR-103R8915. MK is supported under NTU-ERP-102R7701 and NSC 102-2112-M-033-007-MY3. FX is supported under NSC 102-2811-M-002-205, as well as by NSFC under grant No. 11405074. We thank T. Yamanaka for discussions that stimulated this work.

Note Added. During the revision, the long-awaited result of $B_6^{(1/2)}$ appeared [55], extracted from a new lattice calculation carried out by RBC-UKQCD collaboration [56], which indicates a small R_6 .

-
- [1] J.-T. Wei, P. Chang *et al.* [BELLE Collaboration], Phys. Rev. Lett. **103**, 171801 (2009).
 - [2] R. Aaij *et al.* [LHCb Collaboration], Phys. Rev. Lett. **108**, 181806 (2012).
 - [3] T. Aaltonen *et al.* [CDF Collaboration], Phys. Rev. Lett. **100**, 161802 (2008); *ibid.* **109**, 171802 (2012).
 - [4] V.M. Abazov *et al.* [D0 Collaboration], Phys. Rev. Lett. **101**, 241801 (2008); Phys. Rev. D **85**, 032006 (2012).
 - [5] R. Aaij *et al.* [LHCb Collaboration], Phys. Rev. Lett. **108**, 101803 (2012).
 - [6] R. Aaij *et al.* [LHCb Collaboration], Phys. Lett. B **707**, 497 (2012).
 - [7] W.-S. Hou, M. Nagashima, A. Soddu, Phys. Rev. D **76**, 016004 (2007).
 - [8] S.-W. Lin, Y. Unno, W.-S. Hou, P. Chang *et al.* [Belle Collaboration], Nature **452**, 332 (2008).
 - [9] R. Aaij *et al.* [LHCb Collaboration], Phys. Rev. Lett. **111**, 101805 (2013).
 - [10] S. Chatrchyan *et al.* [CMS Collaboration], Phys. Rev. Lett. **111**, 101804 (2013).
 - [11] V. Khachatryan *et al.* [CMS and LHCb Collaborations], arXiv:1411.4413 [hep-ex], accepted to *Nature*.
 - [12] C. Bobeth *et al.*, Phys. Rev. Lett. **112**, 101801 (2014).
 - [13] R. Aaij *et al.* [LHCb Collaboration], Phys. Rev. D **87**, 112010 (2013).
 - [14] Y. Amhis *et al.* [Heavy Flavor Averaging Group], <http://www.slac.stanford.edu/xorg/hfag>.
 - [15] K.A. Olive *et al.* [Particle Data Group Collaboration], Chin. Phys. C **38**, 090001 (2014).
 - [16] CMS Collaboration [CMS Collaboration], CMS-PAS-BPH-13-012.
 - [17] R. Aaij *et al.* [LHCb Collaboration], Phys. Lett. B **736**, 186 (2014).
 - [18] R. Aaij *et al.* [LHCb Collaboration], Phys. Rev. Lett. **114**, 041801 (2015).
 - [19] R. Aaij *et al.* [LHCb Collaboration], Phys. Rev. Lett. **111**, 191801 (2013).
 - [20] C. Langenbruch, talk at Moriond Electroweak 2015, La Thuile, Italy, March 2015.
 - [21] R. Aaij *et al.* [LHCb Collaboration], Phys. Rev. Lett. **113**, 151601 (2014).
 - [22] T. Nomura, talk at ICHEP 2014, Valencia, Spain, July 2014.
 - [23] A. Sergi, talk at ICHEP 2014, Valencia, Spain, July 2014.
 - [24] W.-S. Hou, M. Nagashima, A. Soddu, Phys. Rev. D **72**, 115007 (2005).
 - [25] For a possible interpretation, see e.g. Y. Mimura, W.-S. Hou, H. Kohyama, JHEP **1311**, 048 (2013).
 - [26] W.-S. Hou, M. Kohda, F. Xu, Phys. Rev. D **87**, 094005 (2013).
 - [27] W.-S. Hou, A. Soni, H. Steger, Phys. Lett. B **192**, 441 (1987).
 - [28] The t' mass is large, but always come with CKM factors, hence remains perturbative. The loop functions may be modified by the strong Yukawa coupling, but our purpose to illustrate the power of CKM4 should remain valid.
 - [29] M.S. Chanowitz, M.A. Furman, I. Hinchliffe, Phys. Lett. B **78**, 285 (1978).
 - [30] W.-S. Hou, M. Kohda, F. Xu, Phys. Rev. D **85**, 097502 (2012).
 - [31] S. Aoki *et al.*, arXiv:1310.8555 [hep-lat].
 - [32] W.-S. Hou, M. Kohda, F. Xu, Phys. Rev. D **84**, 094027 (2011).
 - [33] A.J. Buras *et al.*, JHEP **1009**, 106 (2010).
 - [34] K. De Bruyn *et al.*, Phys. Rev. Lett. **109**, 041801 (2012); Phys. Rev. D **86**, 014027 (2012).
 - [35] A.J. Buras, F. De Fazio, J. Girrbach, JHEP **1402**, 112 (2014).
 - [36] A.H. Hoang, A. Jain, I. Scimemi, I.W. Stewart, Phys. Rev. Lett. **101**, 151602 (2008).
 - [37] F. Mescia, C. Smith, Phys. Rev. D **76**, 034017 (2007).
 - [38] A.J. Buras, F. Schwab, S. Uhlig, Rev. Mod. Phys. **80**, 965 (2008).
 - [39] A.V. Artamonov *et al.* [E949 Collaboration], Phys. Rev. D **79**, 092004 (2009).
 - [40] Y. Grossman, Y. Nir, Phys. Lett. B **398**, 163 (1997).
 - [41] J.K. Ahn *et al.* [E391a Collaboration], Phys. Rev. D **81**, 072004 (2010).
 - [42] M. Gorbahn, U. Haisch, Phys. Rev. Lett. **97**, 122002 (2006).
 - [43] G. Isidori, R. Unterdorfer, JHEP **0401**, 009 (2004).
 - [44] A.J. Buras, D. Guadagnoli, G. Isidori, Phys. Lett. B **688**,

- 309 (2010).
- [45] J. Brod, M. Gorbahn, Phys. Rev. Lett. **108**, 121801 (2012).
 - [46] A.J. Buras, M. Jamin, P.H. Weisz, Nucl. Phys. B **347**, 491 (1990).
 - [47] J. Brod, M. Gorbahn, Phys. Rev. D **82**, 094026 (2010).
 - [48] A.J. Buras, J. Girrbach, Rept. Prog. Phys. **77**, 086201 (2014).
 - [49] A.J. Buras, F. De Fazio, J. Girrbach, Eur. Phys. J. C **74**, 2950 (2014).
 - [50] V. Cirigliano, A. Pich, G. Ecker, H. Neufeld, Phys. Rev. Lett. **91**, 162001 (2003).
 - [51] T. Blum *et al.*, Phys. Rev. D **86**, 074513 (2012).
 - [52] An example for a large R_6 value can be found in J. Bijnens and J. Prades, JHEP **0006**, 035 (2000).
 - [53] W. Altmannshofer, D.M. Straub, arXiv:1411.3161 [hep-ph].
 - [54] See B. Dutta, Y. Mimura, arXiv:1501.02044 [hep-ph], for a non-standard supersymmetric model.
 - [55] A. J. Buras, M. Gorbahn, S. Jger and M. Jamin, arXiv:1507.06345 [hep-ph].
 - [56] Z. Bai *et al.*, arXiv:1505.07863 [hep-lat].